Supplementary information

Isotropic imaging across spatial scales with axially swept light-sheet microscopy

In the format provided by the
authors and unedited

SUPPLEMENTARY INFORMATION

Isotropic Imaging Across Spatial Scales with Axially Swept Light-Sheet Microscopy

Kevin M. Dean[1,2*], Tonmoy Chakraborty[3], Stephan Daetwyler[1,2], Jinlong Lin[1,2], Gerard Garrelts[4], Ons M'Saad[5,6], Hannahmariam T. Mekbib[5,6], Fabian F. Voigt[7,8,9], Martina Schaettin[7,8], Esther T. Stoeckli[7,8], Fritjof Helmchen[7,8,9], Joerg Bewersdorf[5,6], and Reto Fiolka[1,2,*]

[1] Department of Cell Biology, University of Texas Southwestern Medical Center, Dallas, TX, USA.
[2] Lyda Hill Department of Bioinformatics, University of Texas Southwestern Medical Center, Dallas, TX, USA.
[3] Department of Physics and Astronomy, University of New Mexico, Albuquerque, NM, USA.
[4] Coleman Technologies, Inc. D.B.A., Sciotex, Newtown Square, PA, USA.
[5] Department of Cell Biology, Yale University, New Haven, CT, USA.
[6] Department of Biomedical Engineering, Yale University, New Haven, CT, USA.
[7] Neuroscience Center Zurich, Zurich, Switzerland.
[8] Department of Molecular Life Sciences, University of Zurich, Zurich, Switzerland.
[9] Brain Research Institute, University of Zurich, Zurich, Switzerland.

Corresponding authors
[*]Kevin M. Dean – kevin.dean@utsouthwestern.edu
[*]Reto Fiolka – reto.fiolka@utsouthwestern.edu

SUPPLEMENTARY METHODS

Sample preparation & imaging of the chicken embryo

Neurofilament staining of a whole-mount chicken embryo: The embryo was sacrificed at day 10 of development and fixed in 4% paraformaldehyde for 3.5 hours at room temperature. For best results, the embryo was kept in constant, gentle motion throughout the staining procedure. Incubations were at 4°C if not stated differently. The tissue was permeabilized in 1% Triton X-100/PBS for 30 hours, followed by an incubation in 20 mM lysine in 0.1 M sodium phosphate, pH 7.3 for 18 hours. Then the embryo was rinsed with five changes of PBS containing 0.2% Triton. To avoid unspecific antibody binding the embryo was incubated in 10% FCS (fetal calf serum) in PBS for 48 hours. The primary antibody mouse anti-neurofilament (1:1'500, RMO270, Invitrogen 13-0700) was added for 60 hours. Unbound primary antibody was removed by ten changes of 0.2% Triton/PBS and an additional incubation overnight. After re-blocking in 10% FCS/PBS for 48 hours, the embryo was incubated with the secondary antibody goat anti-mouse IgG-Cy3 (1:1'000, Jackson ImmunoResearch 115-165-003) for 48 hours. Afterwards, the embryo was washed ten times with 0.2% Triton/PBS followed by incubation overnight. For imaging, the tissue was dehydrated in a methanol gradient (25%, 50%, 75% in H2O and 2x 100%, minimum 4 hours each step at room temperature) and cleared using 1:2 benzyl alcohol: benzyl benzoate (BABB) solution (again gentle shaking is recommended for dehydration and clearing). The tissue and staining are stable for months when kept at 4°C in the dark. This set of animal experiments and procedures were performed in accordance with standard ethical guidelines and were approved by the Cantonal Veterinary Office of the Canton of Zurich.

For imaging, a custom a home-built mesoSPIM mesoscale single-plane illumination microscope (mesospim.org)[21] was utilized. The instrument consists of a dual-sided excitation path using a fiber-coupled multiline laser combiner (405, 488, 515, 561, 594, 647 nm, Omicron SOLE-6) and a detection path comprising an Olympus MVX-10 zoom macroscope with a 1x objective (Olympus MVPLAPO 1x), a filter wheel (Ludl 96A350), and a scientific CMOS (sCMOS) camera (Hamamatsu Orca Flash 4.0 V3). The excitation paths also contain galvo scanners (Scanlab Dynaxis 3M 14-4) for light-sheet generation and reduction of streaking artifacts due to absorption of the light-sheet. In addition, the beam waist is scanned using electrically tunable lenses (ETL, Optotune EL-16-40-5D-TC-L) synchronized with the rolling shutter of the sCMOS camera. This axially scanned light-sheet mode (ASLM) leads to an uniform axial resolution across the field-of-view (FOV) of 4-10 µm (depending on zoom & wavelength). Image acquisition is done using custom software written in Python (https://github.com/mesoSPIM/mesoSPIM-control).

The embryo was mounted in a custom $10 \times 20 \times 80$ mm^3 quartz cuvette (Portmann Instruments). This sample cuvette was then lowered into a custom $40 \times 40 \times 120$ mm^3 imaging cuvette (Portmann Instruments) filled with BABB which allows sample XYZ & rotation movements without refocusing the detection path. Seven tiles covering the embryo were acquired at a zoom setting of 1.25 × (corresponding to a field of view of 10.79 mm / pixel size: 5.27 µm). The laser/filter combinations were: Cy3: 561 nm excitation & 561 nm longpass (561LP Edge Basic, AHF); Autofluorescence: 647 nm excitation & multiband emission filter (QuadLine Rejectionband ZET405/488/561/640, AHF). Imaging data was stitched used BigStitcher[46].

Protocol for Making an Agarose Cube with Fluorescent Particles

     This protocol requires standard wet lab instrumentation, including an analytical balance (30216623, Mettler Toledo), Eppendorf tubes (022363514, Eppendorf), vortex mixer (M16715Q, ThermoFisher Scientific), pipettes and pipette tips (F167360G, Fisher Scientific), and a water purification system (50132370, ThermoFisher Scientific). Additionally, you will need low melting temperature agarose (A9045-25G, Sigma-Aldrich), 200 nm fluorescent beads (17151-10, Polysciences), and a custom agarose mold and holder (CAD diagrams provided). To prepare the fluorescent beads, 1 droplet of the concentrated stock fluorescent bead solution is mixed with 1 mL of deionized water in an Eppendorf tube and vortexed vigorously to eliminate clusters of beads. To prepare a 1% w/w agarose cube, 1 g of agarose is mixed with 100 mL of deionized water, microwaved, and subjected to intermittent stirring until the agarose is completely dissolved into solution. 50 mL of the bead solution is added to 950 mL of the agarose solution in a 1.5 mL Eppendorf tube, mixed vigorously, and then added to the agarose mold for gelation.
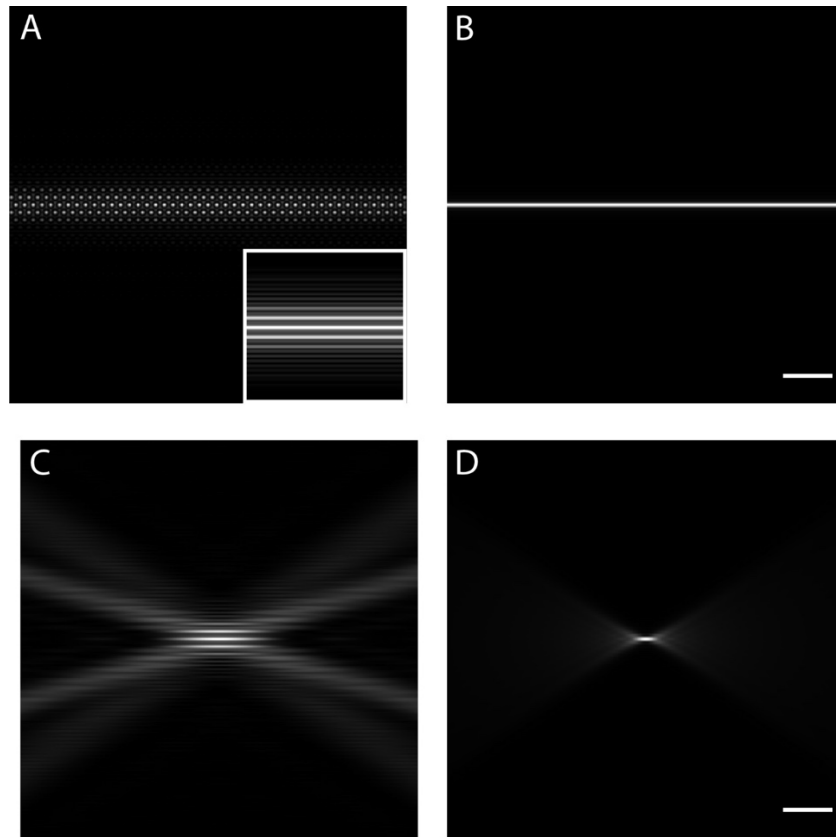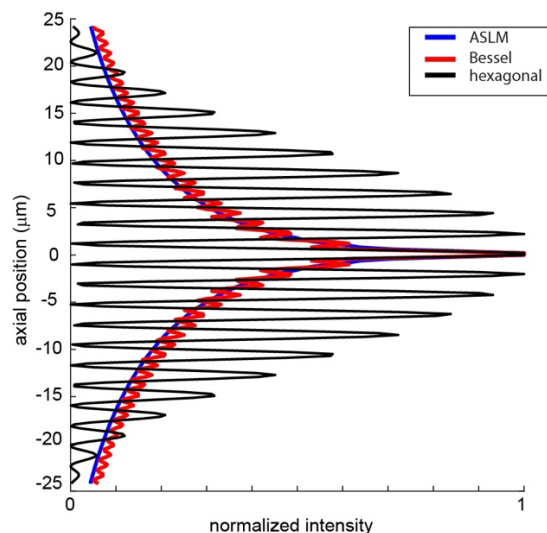
SUPPLEMENTARY FIGURES
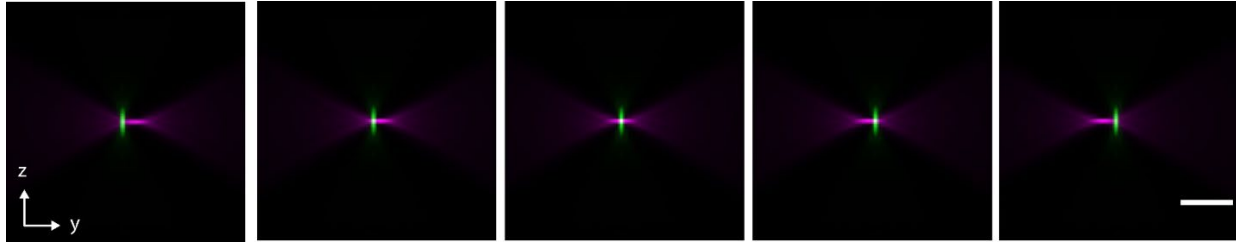
Supplementary Figure 1 - Computation of the Point Spread Function for ASLM. The overall PSF for light-sheet microscopy is the product of the detection Point spread function with the light-sheet intensity distribution. For ASLM, however, during an effective pixel dwell time, the light-sheet is scanned over a finite distance, usually encompassing the length of the beam waist. The simulation above shows the detection PSF in green and the light-sheet in magenta, at five different scan positions of the light-sheet. For each light-sheet position, an instantaneous PSF can computed by taking the product of the detection PSF times the shifted light-sheet. The overall PSF is computed as the sum of the instantaneous PSFs for the different scan positions of the light-sheet. For this numerical simulation, a finite number of PSFs were summed with discrete, pixelated shifts of the light-sheet. Scale Bar: 10 microns.
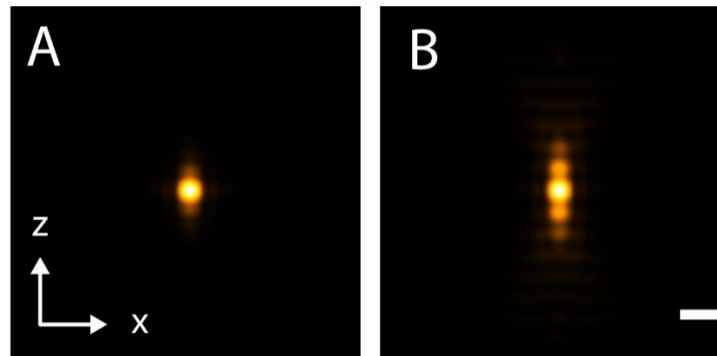

Supplementary Figure 2 - Point spread functions for ASLM and scanned Bessel beam light-sheets. A) Simulated PSF for ASLM with an NA 0.7 for the illumination and detection objective, green fluorescence emission and a rolling shutter width of 24 pixels (4.8 microns). **B)** Simulated PSF for a scanned Bessel beam light-sheet with an NA 0.7 for the illumination and detection objective, green fluorescence emission and a rolling shutter width of 24 pixels (4.8 microns). The simulations were conducted as outlined in Supplementary Figure 1. A gamma correction of 0.8 was applied to both figure panels to better show weaker regions of each PSF. Scale Bar 2 microns

Supplementary Figure 3 – Numerical simulations of hexagonal lattices and Gaussian light-sheets. **A)** Simulated hexagonal lattice patter (inner NA 0.48, outer NA 0.55). Inset shows the corresponding dithered lattice. **B)** Simulated Gaussian light-sheet with the same main lobe thickness as the hexagonal lattice shown in **A)**. **C)** Cross-sectional view of the dithered hexagonal lattice light-sheet shown in **A)**. **D)** Cross-sectional view of the Gaussian light-sheet shown in **B)**. Off note, the amplitude pupil for the Gaussian light-sheet was not Gaussian shaped, but uniform (which is sometimes referred to as a top-hat). This is a more realistic description for our implementations of ASLM, where a physical mask crops the pupil of an overexpanded laser beam. Nevertheless, numerically, a true Gaussian light-sheet (with a Gaussian distribution in its pupil) yields similar results. Scale bars: 10 microns.

Supplementary Figure 4 - Numerical Simulations of illumination intensities for ASLM, scanned Bessel beam and hexagonal lattice light-sheets. Each light-sheet was simulated in 3D using vectorial Debye theory for electromagnetic fields. For ASLM, first a Gaussian light-sheet with equivalent main lobe thickness to the main lobes of the Bessel and hexagonal lattice was computed. Off note, the amplitude pupil for the Gaussian light-sheet was not Gaussian shaped, but uniform (which is sometimes referred to as a top-hat). To create the ASLM intensity, the Gaussian light-sheet was numerically scanned over a distance of 100 microns. For both the Bessel beam as well as the hexagonal lattice, the annulus was chosen such that they resulted in a propagation length of a hundred microns as well. To obtain a simulation of a light-sheet, both the Bessel beam as well as the hexagonal lattice were numerically scanned laterally. The displayed cross-sectional intensity profiles were measured in the center of each light-sheet.
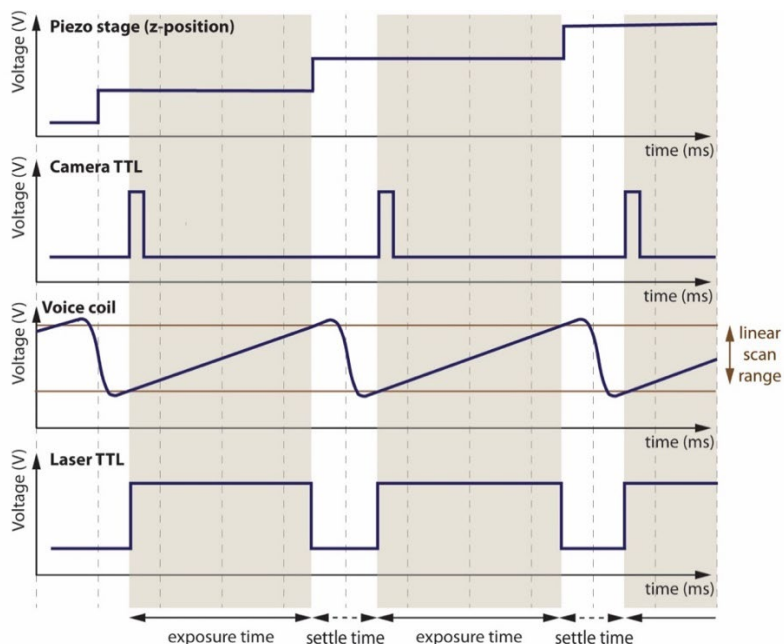
Supplementary Figure 5 – Key analog outputs for driving a sample scanning variant of ASLM. (Top): drive signal for the piezo stage that translates the sample. (second from Top): The camera is triggered by the rising edge of the TTL signal. (third from Top): The actuator for the remote mirror is driven with a sawtooth signal that has short fly back portion and also smoothing of the sharp edges. The actual camera exposure occurs during the linear ramp portion of the signal. (Bottom): The laser is triggered such that the sample is only illuminated during the exposure time of the camera. On the time axis, within "settle time", the piezo stage settles for its new position, the actuator for the remote focusing mirror flies back to the starting position and the camera is read out.

SUPPLEMENTARY TABLES

Supplementary Table 1 – Key Optical Components for a Cost-Effective Live-Cell Variant of ASLM.

Optical Component or Parameter	Cost-Effective ASLM
Entry Beam Size ($1/e^2$)	12 mm
HWP	Half Wave Plate
L1	50 mm Cylindrical Lens
L2	80 mm Achromatic Doublet
L3	60 mm Scan Lens
L4	200 mm Tube Lens
PBS	Polarizing Beam Splitter
QWP	Quarter Wave Plate
Remote Focusing Objective	Nikon 40x NA 0.8 Water Dipping Objective
L5	200 mm Tube Lens
L6	200 mm Tube Lens
Illumination Objective	Nikon 40x NA 0.8 Water Dipping Objective
Detection Objective	Nikon 40x NA 0.8 Water Dipping Objective
L7	200 mm Tube Lens

Supplementary Table 1 – The original ASLM variant described here used a linear mirror galvanometer pair to rapidly dither the beam laterally for shadow reduction and scan the beam in the z-dimension synchronously with the piezo mounted detection objective. Thus, the entire system operated in a laser scanning format (see also Figure 6b for lens numbering).

Supplementary Table 2 – Key Optical Components for a High-NA Live-Cell Variant of ASLM.

Optical Component or Parameter	Cost-Effective ASLM
Entry Beam Size ($1/e^2$)	2.1 mm
HWP	Half Wave Plate
L1	50 mm Cylindrical Lens
L2	75 mm Achromatic Doublet
L3	60 mm Scan Lens
L4	100 mm Achromatic Doublet
PBS	Polarizing Beam Splitter
QWP	Quarter Wave Plate
Remote Focusing Objective	Nikon 40x NA 0.6 Air Immersion Objective (CFI Plan Fluor ELWD)
L5	100 mm Achromatic Doublet
L6	200 mm Tube Lens
Illumination Objective	Special Optics NA 0.71 Water Immersion Objective (54-10-7)
Detection Objective	Nikon 25x NA 1.1 Water Immersion Objective (CF175 Apo LWD)
L7	500 mm Achromatic Doublet

Supplementary Table 2 - The original ASLM variant described here used a linear mirror galvanometer pair to rapidly dither the beam laterally for shadow reduction and scan the beam in the z-dimension synchronously with the piezo mounted detection objective. Thus, the entire system operated in a laser scanning format (see also Figure 6a for lens numbering).

Supplementary Table 3 – Key Optical Components for a Large Field of View ctASLMv1.

Optical Component or Parameter	Cost-Effective ASLM
Entry Beam Size $(1/e^2)$	14 mm
HWP	Half Wave Plate
L1	50 mm Cylindrical Lens
L2	200 mm Achromatic Doublet
PBS	Polarizing Beam Splitter
QWP	Quarter Wave Plate
Remote Focusing Objective	Nikon 20x NA 0.7 Air Immersion Objective (CFI60 Super Plan Fluor LWD)
L3	150 mm Achromatic Doublet
L4	250 mm Achromatic Doublet
Illumination Objective	ASI NA 0.4 Multi-Immersion Objective (54-10-12)
Detection Objective	ASI NA 0.4 Multi-Immersion Objective (54-10-12)
L5	200 mm Tube Lens

Supplementary Table 3 – ctASLM operates in a sample scanning format (see also Figure 6b for lens numbering), which reduces the cost and complexity of the optical setup by eliminating the need for a mirror galvanometer pair and a scan lens. For shadow reduction a resonant galvo is placed at the focus of the cylindrical lens.

Supplementary Table 4 – Key Optical Components for High-Resolution ctASLMv2.

Optical Component or Parameter	Cost-Effective ASLM
Entry Beam Size $(1/e^2)$	11 mm
HWP	Half Wave Plate
L1	50 mm Cylindrical Lens
L2	100 mm Achromatic Doublet
PBS	Polarizing Beam Splitter
QWP	Quarter Wave Plate
Remote Focusing Objective	Nikon 20x NA 0.7 Air Immersion Objective (CFI60 Super Plan Fluor LWD)
L3	125 mm Achromatic Doublet
L4	150 mm Achromatic Doublet
Illumination Objective	ASI NA 0.7 Multi-Immersion Objective (54-12-8)
Detection Objective	ASI NA 0.7 Multi-Immersion Objective (54-12-8)
L5	300 mm Achromatic Doublet

Supplementary Table 4 – ctASLM operates in a sample scanning format (see also Figure 6b for lens numbering), which reduces the cost and complexity of the optical setup by eliminating the need for a mirror galvanometer pair and a scan lens. For shadow reduction a resonant galvo is placed at the focus of the cylindrical lens.

Supplementary Table 5 – Key Optical Components for a mesoSPIM V5

Optical Component or Parameter	mesoSPIM V5
Fiber-coupled laser engine	Omicron SOLE or Omicron Lighthub or Toptica MLE with either 1 or 2 output fibers (# of excitation directions)
Collimator	60 mm Achromatic Doublet
Electrically tunable lens	Optotune EL-16-40-TC-VIS-5D-1-C
Relay lenses	2x 80 mm Achromatic Doublets
Galvo scanners	Thorlabs GVS211/M
Excitation Objective	Nikon AF-S Nikkor 50 mm f/1.4G
Detection Path	Olympus MVX-10 Macroscope with MVPLAPO 1x objective
Filter wheel	Ludl 96A350 with MAC6000 controller
Camera	Hamamatsu Orca Flash V3
Stages	mesoSPIM stage kit (Physik Instrumente M-900K276)

Supplementary Table 5 – Due to its low excitation NA of 0.1, the mesoSPIM utilizes electrically tunable lenses instead of a remote focusing path. The light-sheet is generated by scanning a gaussian beam using galvo scanners.
For detailed parts lists and documentation please see http://mesospim.org and https://github.com/mesoSPIM

Supplementary Table 6 – Recommended Computer and BIOS Configuration.

Item	Qty	Cost	Notes
SXT9800 Workstation	1	$3,500	Available from Colfax International.
Intel Xeon Silver 4210R 10C/20T	2	$1,100	Can upgrade to higher performance CPUs
16GB of 2.9GHz DDR4 RAM	12	$1,800	Can decrease to 8GB RAM for total capacity of 96GB.
Micron 7300 Max 800GB M.2 NVMe Drive	1	$230	Fast SSD for operating system.
Intel D3 S4510 Series 8GB SSD	1	$1900	Fast SSD for reading and writing data.
Intel X5540-T1 10G Network Card	1	$350	Useful for transferring data to the server. Faster and slower options available, consult with your IT department for supported networking options.
NVIDIA Tesla Pascal P40 24GB GPU	1	$6,500	Optional. Only necessary for rendering data with advanced software. Motherboard sufficiently powerful for standard display functions.
Logitech K800 Wireless Illuminated Keyboard + M705 Mouse	1	$90	Back illuminated useful for working in the dark.
StarTech PEX4S553B 4 Port RS232 PCIe Serial Card	1	$80	Necessary for control of stages, filter wheels, etc.
24” Monitor	1	$150	If using built in graphical capacity of motherboard, requires VGA connection.
PCIe-7852	1	$5200	FPGA for instrument control
SCB-68A	1	$350	Terminal block for BNC cables
SHC68-68-RMIO Shielded Cable	1	$180	Cable for terminal block
Total Cost		$7,000 - 16,000, depending on configuration.	

Supplementary Table 6 - Design of Microscope Acquisition Computer. We recommend the ProEdge SXT9800 Workstation from Colfax International, which provides a powerful and large capacity motherboard with 6 PCIe 3.0 x16 slots. The layout of such a computer is massively customizable, and given the rapid pace of computer development, the costs below are approximate, and better options are likely available. We recommend consulting with Colfax International who provide incredible support in the design of a tailored computer system. We also suggest that all energy savings be disabled on the computer, and that the BIOS be configured such that C-State control and hyperthreading are disabled, Turbo Boost Technology is enabled, and SpeedStep be automatic.

Supplementary Table 7 – Necessary Software and Approximate Cost.

Software and Hardware	Cost	Location
DCAM-API	$0	https://dcam-api.com/
Microsoft .NET Framework	$0	https://dotnet.microsoft.com/download/dotnet-framework
Fiji (or ImageJ)		https://fiji.sc
PI MikroMove	$0	https://www.pi-usa.us/en/products/controllers-drivers-motion-control-software/motion-control-software/
LabVIEW 2016, 64-bit.	$3,000	https://www.ni.com/en-us/support/downloads
LabVIEW 2016 Run-Time Engine	$0	https://www.ni.com/en-us/support/downloads
LabVIEW NI-RIO Drivers	$0	
LabVIEW Real-Time Vision Development Bundle	$2,000	
NI Vision Development Module Run-Time License	$110	
Total Cost for Full Development System	**$5000**	
Total Cost for Executable System	**$110**	

Supporting Table 7 – Software Necessary for Instrument Control. Costs are approximate and assume academic pricing.

Supplementary Table 8 – Microscope Wiring for Laser Scanning Variant.

| Channel Description	Channel
Shutter	DIO3
Camera External Trigger	DIO4
Camera Fire Output	DIO8
Laser 0	AO5
Laser 1	AO6
Laser 2	AO7
Laser 3	AO3
Sample Scanning Piezo	AO0
Remote Focusing Position	AO1

Supporting Table 8 – Wiring diagram of ASLM. All outputs are delivered via the NI 7852R FPGA through the 'Connector0' output. Exact pinouts of the data acquisition hardware can be found using the NI MAXX program under "Devices and Interfaces." Right-click on your device and select "Device Pinouts".

Supplementary Table 9 – Microscope Wiring for Sample Scanning Variant.

Channel Description	Channel
Shutter	DIO3
Camera External Trigger	DIO4
Camera Fire Output	DIO8
Laser 0	AO5
Laser 1	AO6
Laser 2	AO7
Laser 3	AO3
Sample Scanning Piezo	AO0
Remote Focusing Position	AO1

Supporting Table 9– Wiring diagram of ASLM. All outputs are delivered via the NI 7852R FPGA through the 'Connector0' output. Exact pinouts of the data acquisition hardware can be found using the NI MAXX program under "Devices and Interfaces." Right-click on your device and select "Device Pinouts".

SUPPLEMENTARY NOTES
Supplementary Note 1 – Operating the Image Acquisition Software.

The image microscope control software is available as source code and as an executable (e.g., precompiled binary) that can be deployed on any Windows machine that is equipped with the proper LabVIEW dependencies (See Supplementary Tables 6 and 7). Upon completion of an MTA, this software is freely available and can be cloned via GIT. The executable file is located at /lightsheet/bin/LouisXIV.exe, and the initialization file, which is used to preconfigure the microscope, is located at /lightsheet/SPIM/SPIM Support files/SPIMProject.ini. Several parameters within this initialization file can be modified via the software's GUI, and a functioning initialization file is available via the AdvancedImagingUTSW GitHub repository. The GUI provides a simple interface for users to control microscope operation and is organized in a tabular format. On the left-hand side of the GUI, one configures the scan and acquisition parameters, and the right side provides an intuitive display of the image and waveforms driving the microscope. The mode of operation (Continuous Scan, Z-Stack, and Single Image) can be adjusted via the pull-down menu on the top-left. The acquisition is initiated by pressing the 'Acquire' button, and the overall progress towards completion is provided in the continuously updating progress bars.

The image window allows one to immediately gauge the brightness of the sample via the Max Counts display. For fast acquisitions, where it can be difficult to observe the rapidly changing max counts, a rolling 'Frames to Avg' option is available. Further to the right, one can save the image straight to disk, pop out an additional image window with the 'Cam1' button, perform maximum intensity projections from each image perspective (e.g., XY, XZ, and YZ) with the 'Projections' button. One can also change the lookup table, add a scalebar, zoom in and out, autoscale the lookup table or specify the exact counts desired in the lookup table. Lastly, you can also embed text information into the image, which is useful for timestamping the data more directly.
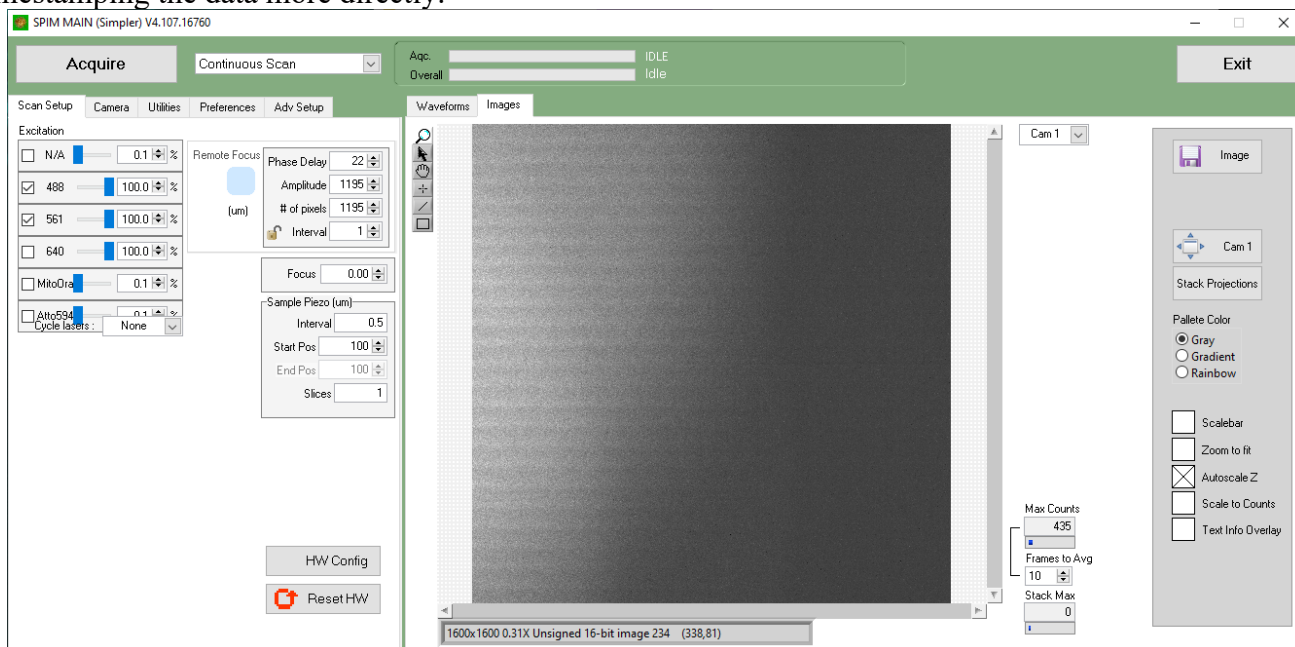

Under the Scan Setup tab, the illumination sources desired are selected. If your laser sources accept analog modulation, their operating power can be adjusted from 0-100%. Otherwise, the lasers can be digitally modulated by simply placing the intensity at 100%, which sends the user-specified maximum voltage to the light source (usually 5V). Immediately below the lasers is a dropdown menu that allows the user to specify how they would like to cycle the lasers (more information below). Adjacent to the laser subpanel is the control for remote focusing. This includes a method for adjusting the phase of the remote focusing sawtooth waveform, the amplitude of the sawtooth waveform, and the digitization of the waveform (e.g., # of pixels and interval). A greater number of 'pixels' allows you to digitize the waveform more finely, but at the cost of additional computational overhead.

Located on the bottom of the left panel is an option for resetting the hardware, which is useful for resolving communication issues with peripheral devices (e.g., filter wheels and stages). Adjacent to this is the HW Config button, which allows you to configure the camera serial number, image transformation, binning, and model for multiple cameras. Although not discussed in detail here, additional cameras can be configured to operate in a 'Remote' mode via a dedicated 10G network switch, thereby allowing you to overcome hardware limitations associated with housing numerous resource intensive frame grabbing devices in a single computer. By pressing the HW Config button, a new GUI window becomes available for programming the microscope.

The camera settings are accessible via the Camera tab on the left-hand side. Here, the exposure is configured, and camera sensor mode. This allows you to toggle between standard camera operation and the light-sheet mode, as well as control the width of the rolling shutter and direction (e.g., from top to bottom, or vice versa) of its sweep. The field of view is specified via the ROI interface, and the framerate is automatically calculated according to the exposure time and ROI-dependent readout time.
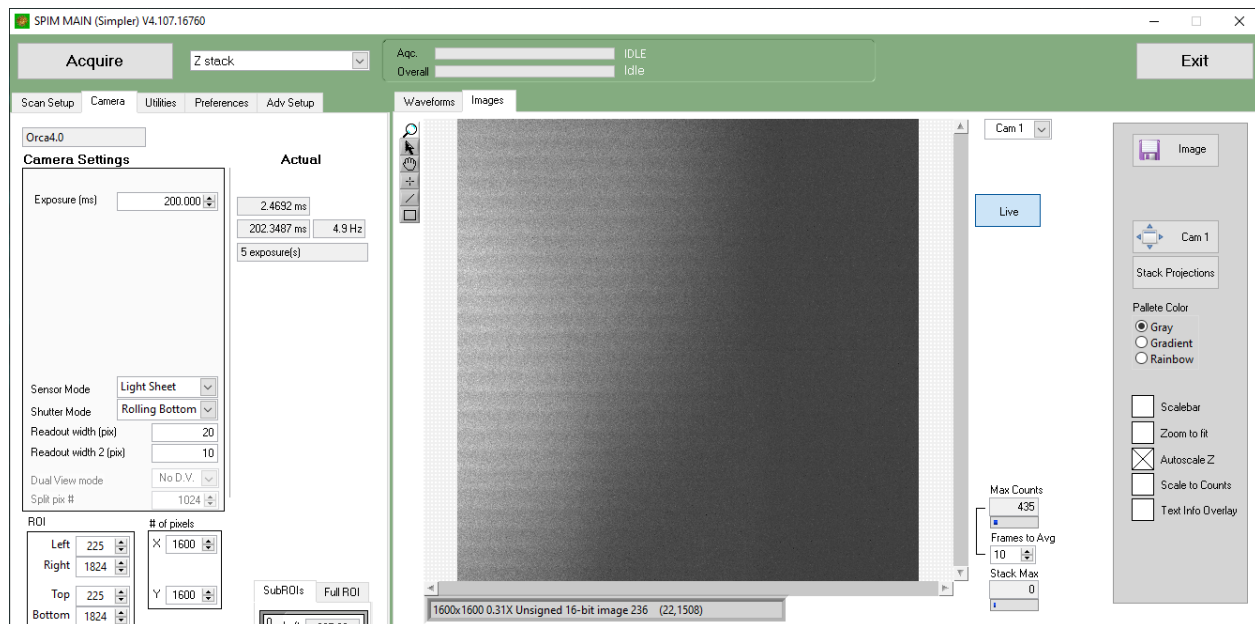
It is often advantageous to visually confirm that the waveforms for driving the microscope are correct. Here, we show a hypothetical z-stack acquisition. Importantly, as can be seen on the left, additional options are available for a z-stack that include the starting position of the stack, the ending position of the stack, and the stack interval (e.g., distance between adjacent images). Further, one can also specify whether one wants to acquire a single timepoint, or multiple. For the latter, the user can specify a timepoint delay. Here, we created a single timepoint z-stack with 5 slices and two lasers, which makes it easy to visualize the waveform. The top waveform is a zoom in of the remote focusing sawtooth signal, which includes a linear ramp and return, as specified by the remote focusing amplitude, phase delay, and more advanced parameters such as a smoothing and flyback parameter (more below). The Cycle Lasers parameters is set as per Z, which means that for every image plane, each laser will individually be toggled, and an image will be acquired. In the bottom panel, one can see that the remote focusing waveform is repeated 10x. Thus, for each Z position, each laser is toggled sequentially (shown as AOTF0 and AOTF1).
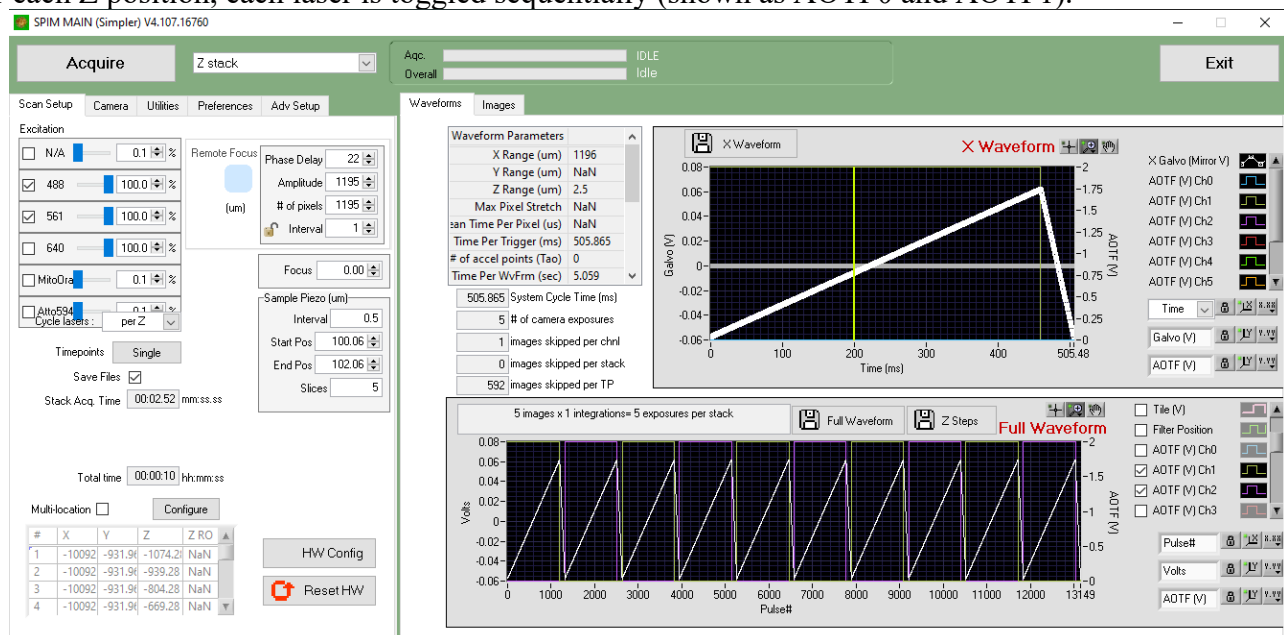

In the per Stack mode, the first laser is triggered 5 times as the sample is scanned in Z, then the sample is repositioned at the starting point, and the second laser is triggered 5 times as the sample is scanned in Z. Operation in this mode is useful if operating with slower devices, such as filter wheels. Other

microscope components can also be readily visualized (e.g., the filter wheel position, z-position, etc.) using this interface.
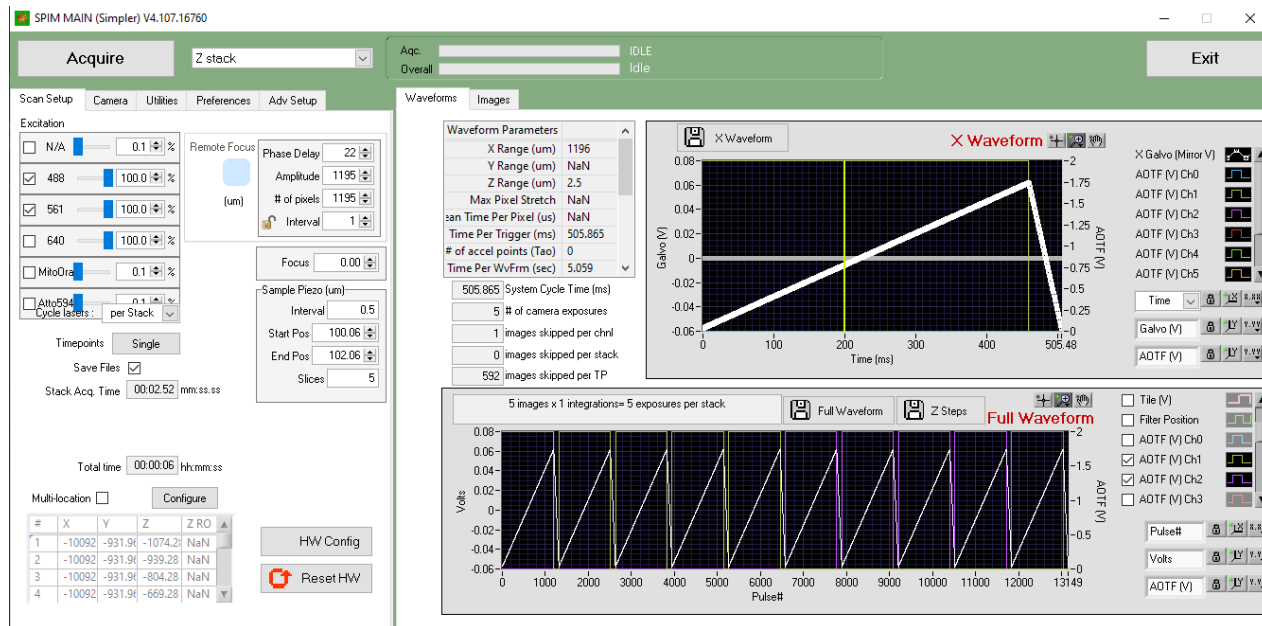

Additional configuration parameters are available under the preferences tab. Here, we recommend that the settings are restored on startup. One can also select different file types to save the data to, including .tiff, .raw., and .bigTIFF. The latter two are useful for acquiring z-stacks that are larger than ~4.7GB as can readily occur imaging large chemically cleared specimens with fine z-sampling. If the user specifies tiff, then they can choose to embed the industry standard OME-XML metadata into the file. Lastly, the user can also specify the minimum and maximum RAM buffer size. Of note, one can buffer a large amount of RAM, but there is a performance falloff owing to the large number of memory locations that must be handled. As such, we recommend buffering ~200-300 image volumes, maximum. The 'Adv Setup' tab allows one to adjust low-level parameters, such as the aforementioned smoothing and fractional flyback parameters for the remote focusing waveform, and the custom cycle time parameter, which can be used to lengthen the acquisition time window.
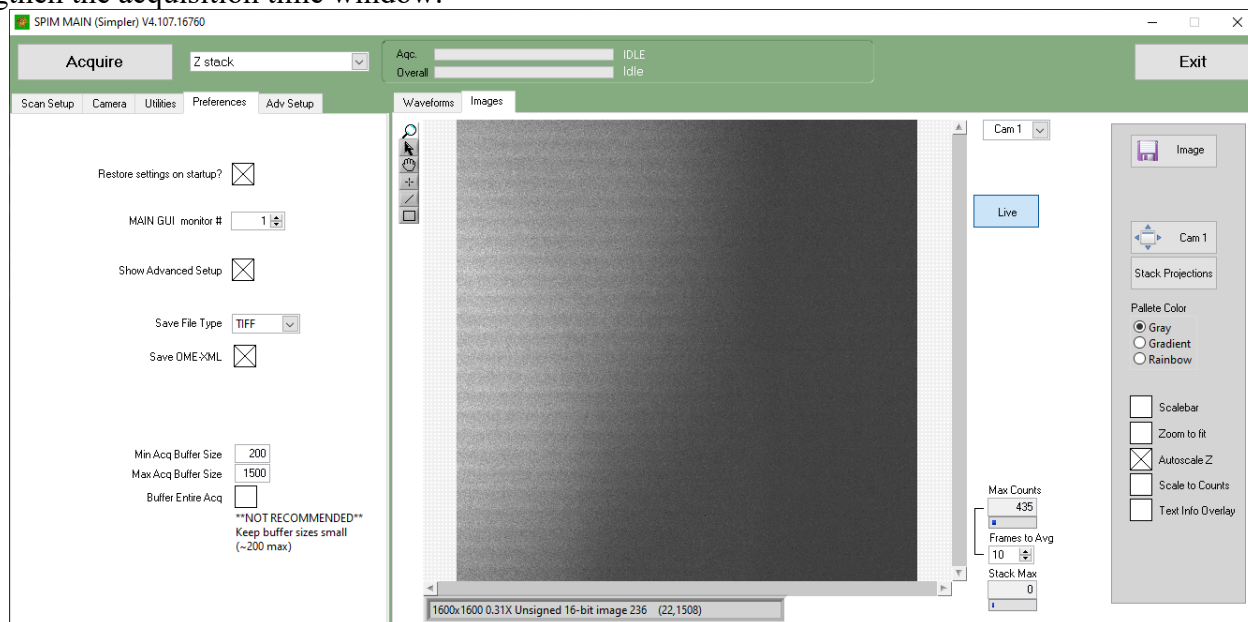
For cleared tissue imaging, the specimen is often larger than the field of view, which requires image tiling or the acquisition of different image volumes in an automated fashion. On the z-stack tab, one can select the 'multi-location' textbox to enable stage control, and the 'configure button to create a new GUI

element for doing so. The Sample Stage Control GUI allows one to configure the stage-specific parameters (e.g., scan rate, settling time, COM port, baud rate, axis definition, etc.) and also provides the current stage location. Potential regions of interest can be saved to the 'Saved Locations' queue, and if desired, can be moved to the 'Location Sequence' queue for automated imaging. If image tiling is desired, one selects the 'Gen. Grid Sequence', located in the bottom-right of the Sample Stage Control GUI.
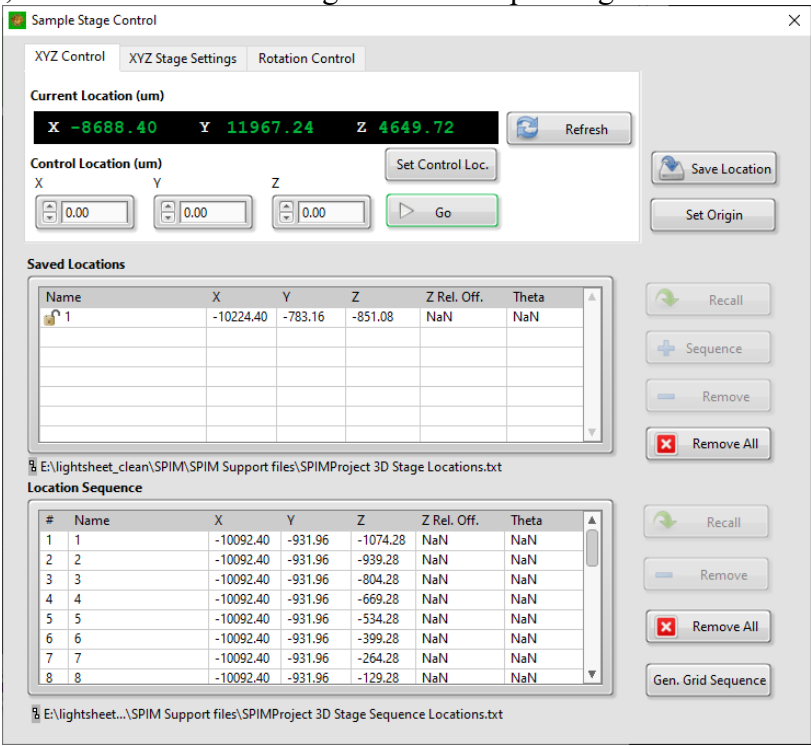
The Generate Multipoint Grid Sequence GUI allows one to specify a cubic volume with absolute or relative volume dimensions. The overlap between adjacent volumes is specified, and the entire tiling progression is automatically created by pressing the 'Generate Grid Sequence', which can be moved to the sample stage control GUI by pressing the 'Set Sequence' button.

Supplementary Note 2 – Useful Approaches for Aligning Optics.

Laser Safety.

As with any optical system that uses lasers, one must follow appropriate safety guidelines. We recommend regular communication with a laser safety officer, appropriate laser safety training, protective eyewear, proper signage, and laser interlock systems as some, but not all, steps for ensuring laser safety.

General Strategies.

The hole pattern of an optical table is a useful guide for the laser beam and serves as convenient measure for how linear the laser beam is propagating. Irises, or alignment business cards, can be placed on the hole pattern for evaluation of beam trajectory. We also recommend that mirrors reflect the beam at 90 degrees. It is also useful to use a common beam height throughout the microscope build. We use a 3-inch beam height, which is conveniently confirmed with a magnetic ruler (ThorLabs, BHM1) that offers 2 mm apertures at both 25 mm and 1-inch increments. To minimize vibrations and thermal drift, we rigidly mount optics on 25 mm diameter pedestal pillar posts (ThorLabs, RS2.5P8E). It is also important to practice laser safety in accordance with the American National Standards Institute to minimize the possibility of injury.

Laser Beam Walking

After mounting the laser to the optics table, it is necessary to get the beam to the desired height and direction, e.g., along the hole pattern. To achieve this, introduce two kinematically mounted mirrors (ThorLabs, PF10-03-F01, and POLARIS-K1), each at 45 degrees, immediately after the laser. An initial crude alignment to get the beam following the hole pattern requires both translation, and rotation, of the mirror mounts. Linear propagation in both the horizontal and vertical directions can be evaluated by checking the beam position immediately after the second mirror, and ~1-2 meters away from it. Adjustment of the first mirror can be used to 'walk' the laser towards the desired position immediately after the second mirror, and adjustment of the second mirror can be used to 'walk' the laser beam towards an alignment

target ~1-2 meters away from it. This procedure is iterated until an optimal beam alignment is found and the beam propagates linearly down the hole pattern on the optical table.

Optical Back Reflections.

When introducing lenses into an optical system, the performance of the lens depends critically on the positioning of the lens both laterally and rotationally relative to the incoming beam. To evaluate lens position, we decrease the diameter of the incoming beam with a concentric iris, place a business card with a small diameter hole punched into it (or burned with a soldering iron) just prior to the lens being introduced, and optimize the back scattered light from the first and second glass interfaces so that they are concentric with the aperture. A perfectly aligned lens will produce concentric backscatter. Lenses can be placed in a 4f telescope geometry to adjust the illumination beam diameter, or to improve the laser profile with a spatial filter. Here, not only is it important to optimize the orientation of lenses, but the distance between them. When the telescope is properly aligned, the beam will be well collimated, and will continue straight along the hole pattern. A useful way to evaluate beam collimation is with a shear plate interferometer (ThorLabs, SI035). A perfectly aligned, high-quality beam, results in linear fringes.
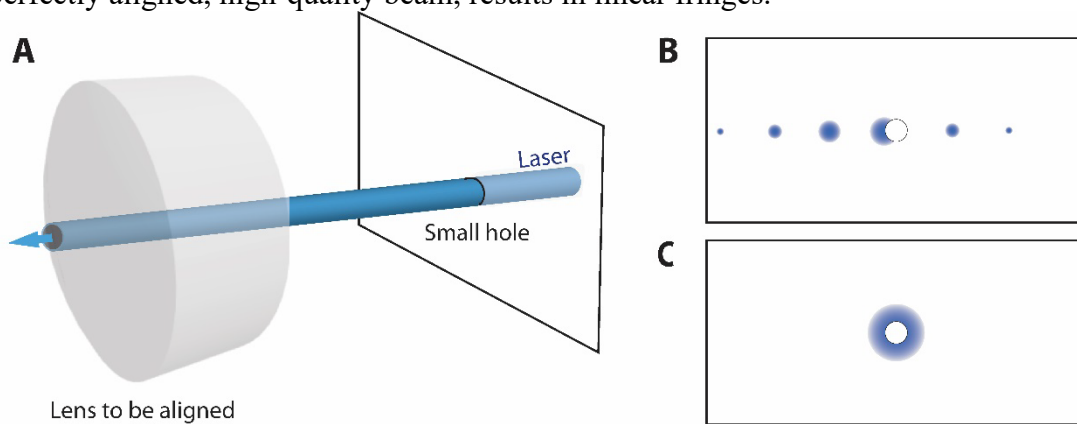
Coherent Backscatter at a Laser Focus

It is often useful to know where the exact position of the laser focus is, particularly for construction of spatial filters and for the introduction of scanning components (e.g., galvanometers). Place the business card immediately adjacent to the laser light such that you can see the backscattered light. Translate the semi-reflective surface along the laser propagation direction and pay attention to the backscattered light. When the laser is maximally focused, a coherent pattern with large features will be evident on the business card with the reflected light.

*Measuring Collimation with a Shear Plate Interferometer.*

A shear plate interferometer consists of an optical flat positioned at 45 degrees relative to the optical path which reflects laser light towards a diffuser. An incoming collimated laser is reflected towards the diffuser at the first and second surfaces of the optical flat, which introduces a path-length difference that manifests as an interference pattern on the diffuser. When perfectly collimated, the interference pattern will consist of a series of linear stripes with the stripes aligned along the optical path of the incoming laser beam. In contrast, converging and diverging beams will have a rotated stripe pattern. Conveniently, other types of aberrations, including coma, spherical, and astigmatism, manifest as non-linear stripes. For proper function, the shear plate must be matched to the incoming beam dimensions. As a note, not all lasers will produce fringes with good visibility on a shear-plate. This has to do with the coherence length, which might be exceeded by the path difference between the first and second reflection from the optical flat. We noticed that some diode pumped solid state lasers, such as the OBIS lasers sold by Coherent Inc. used in some of our ctASLM setups, can produce visible fringe pattern at very low power settings, which disappear when power is increased.

Laser Alignment Module

There are certain instances where measuring the back-reflections with the illumination beam is not possible. One such example is when one is aligning the detection path of a light-sheet microscope. Here, it is convenient to have an alignment module which allows you to precisely introduce a small diameter laser beam into the optical path. To achieve this, we use a laser alignment module that was developed by the Gustafsson lab (CAD provided here: https://github.com/AdvancedImagingUTSW/manuscripts/tree/main/2021-dean-protocol). This module is designed to be installed using a standard objective thread size and allows one to measure the back-reflections on optical components downstream. Set screws are used to align the alignment module using the protocol reported by Abrahamsson et al[47].

Supplementary Note 3 – Assembly of the Sample Immersion Chamber.

As described in this manuscript, the entire optical system is assembled horizontally on an optical table. Accordingly, the specimen is positioned vertically in a large chamber at the intersection of the illumination and detection objectives (a CAD drawing is provided online at https://github.com/AdvancedImagingUTSW/manuscripts/tree/main/2021-dean-protocol). The chamber is machined from aluminum or 3D printed with acrylonitrile butadiene styrene (ABS) and smoothed with acetone. To seal the chamber, and fully embed the specimen within imaging media, we cut a small ~5 mm diameter aperture into a 1/32" thick super-soft silicone sheet (e.g., 9010K81 from McMaster-Carr, or 1MWJ1 from Grainger) and press this membrane against the chamber using circular compression plates. The objectives are then introduced through the small aperture in the silicone sheet. If the hole in the silicone membrane is too small, objective scanning may be problematic due to the increased tension. Conversely, if the hole is too large, the chamber will leak. Some optimization is to be expected depending upon the dimensions of the illumination and detection objectives.
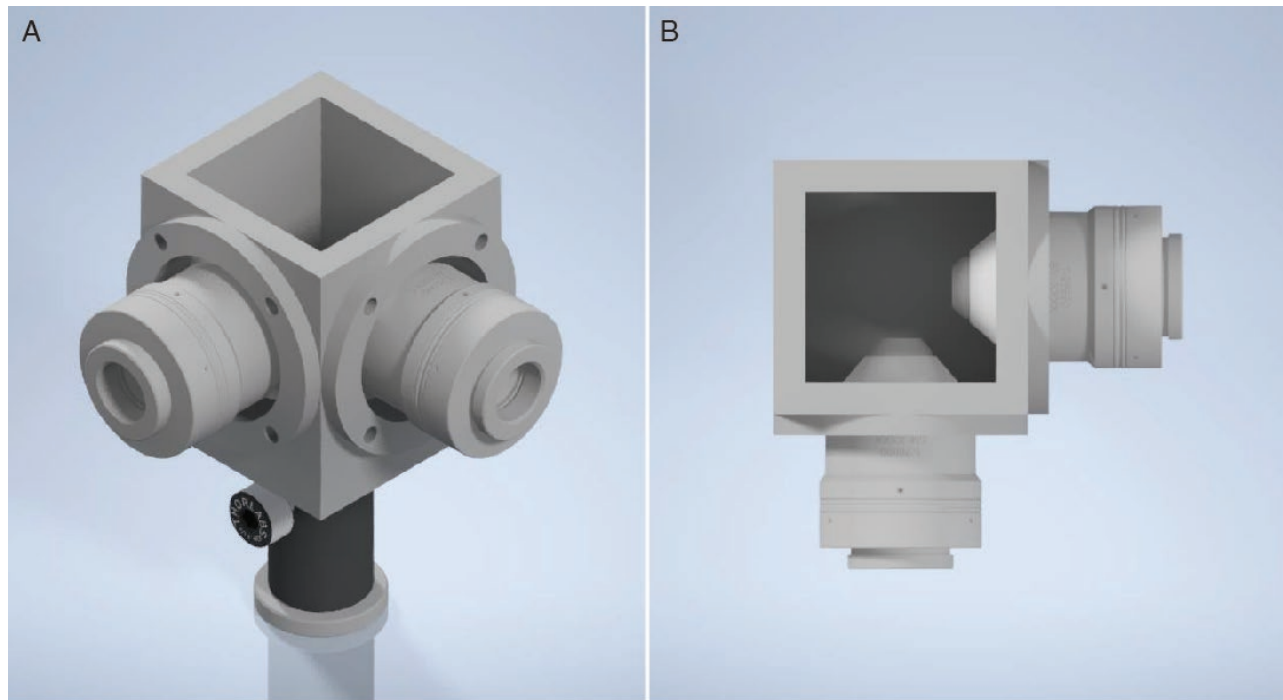
**Supplementary Note 4 – Assembly of the Sample Mounting System.**

There are several different methods for assembling a sample mounting system. For ctASLM, we adopted a simple approach that combines a 3D stage (e.g., Sutter 3DMS) with 25 mm of optical travel for tiling, and a linear stage (e.g., a voice coil or piezo) for precision scanning of the sample through the focus. While the second stage is redundant, it provides a much faster response and is more accurate than the large travel range tiling stage. In the provided example (see https://github.com/AdvancedImagingUTSW/manuscripts/tree/main/2021-dean-protocol), these two stages are connected through a custom machined adapter. On the front of the linear stage a second adapter (shown in black) holds a u-shaped bracket (shown in red), which when combined with a set screw, allows the sample to be hung vertically into the imaging chamber. This approach allows rapid vertical movement of the specimen through the adjustment of a single screw. At the base of an extension, a second bracket (gray, bottom) again uses a set screw to hold a coverslip with the sample glued to it in position. Of note, for optimal microscope performance, the coverslip should be mounted at 45 degrees relative to the illumination and detection optical paths. If the optical cone of illumination light traverses the optical coverslip prior to the specimen, or the optical cone of the resulting fluorescence traverse the glass prior to reaching the detection objective, it will be severely aberrated.
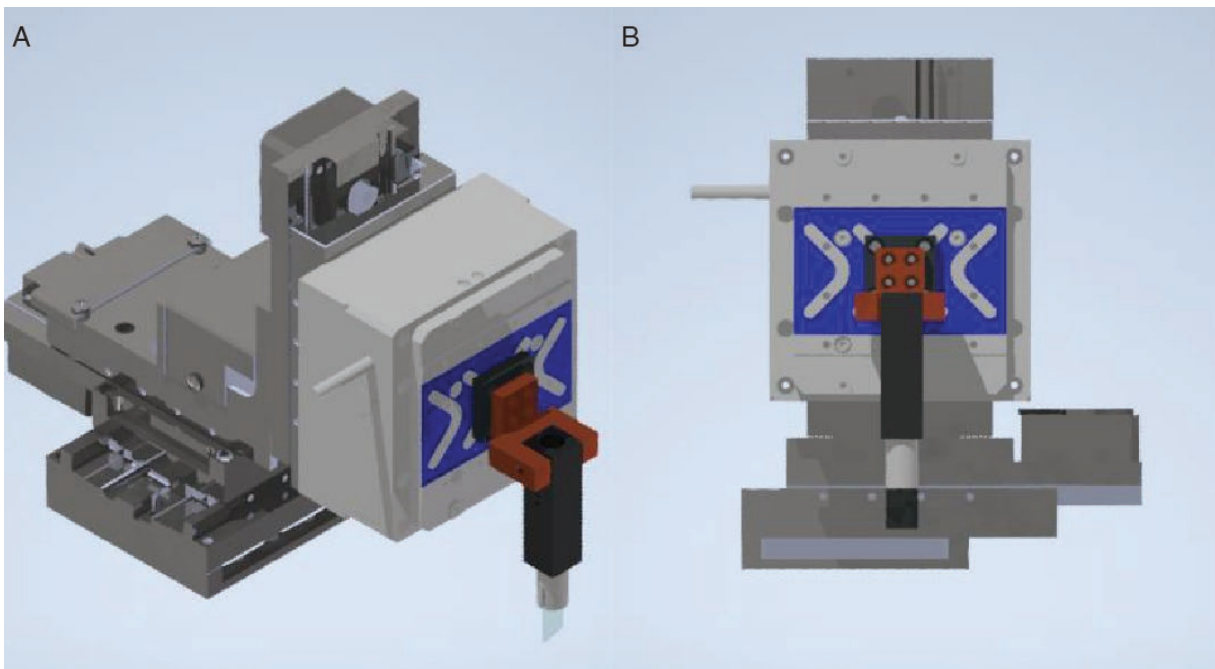
Supplementary Note 5 – Casting an Agarose Cube for Resolution Measurements.

Sub-diffraction nanospheres are the gold standard for measuring the resolution of an optical system. While fluorescent nanospheres can be adhered to a 2D glass coverslip using poly-l-lysine, it is much more convenient to have a 3D target for performing 3D resolution measurements. To achieve this, we prepare agarose cubes with fluorescent nanospheres embedded (e.g., 17151-10, Polysciences). The agarose cube is made using a molding system consisting of two custom machined plates and an agarose mount, all held together with 8-32 socket head screws (see https://github.com/AdvancedImagingUTSW/manuscripts/tree/main/2021-dean-protocol). Cumulatively, they create a ~5x5x5 mm void, which a 1% (w/w) molten agarose solution mixed with dilute fluorescent nanospheres can be pipetted into. The agarose mount features protruding features which the molten agarose encapsulates and upon gelation of the agarose, secures it in place. The entire agarose mount is then removed from the molding system with the agarose cube attached and placed where the coverslip mounting bracket is shown in **Supplementary Note 3**. Here, the flat faces of the cube are positioned along the optical axes of the illumination and detection paths. Of note, too high of a concentration of agarose can result in spherical aberrations owing to an increased refraction index difference between the immersion media and the agarose. Alternatively, too low of a concentration of agarose results in a mechanically unsound agarose cube.
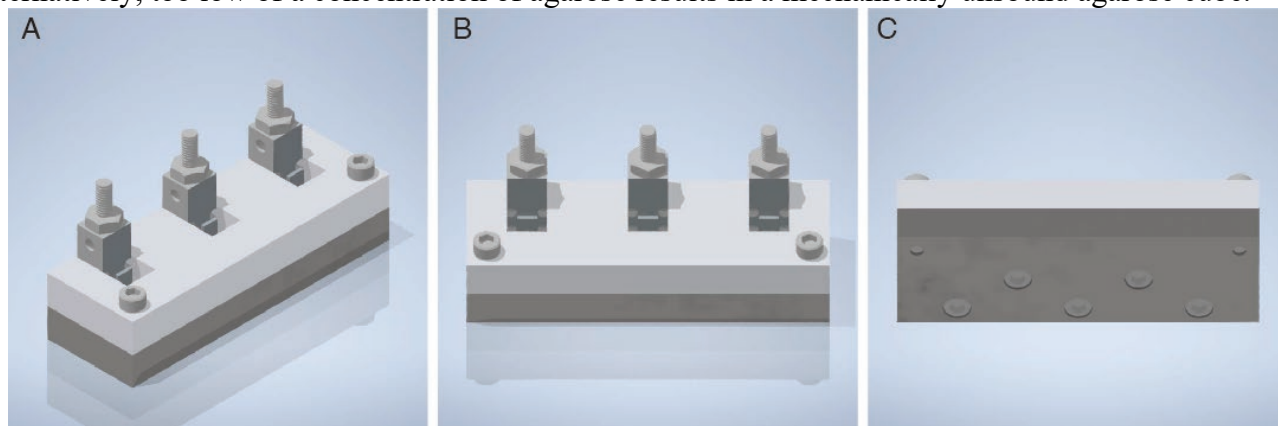
Supplementary Note 6 – Quantitative Evaluation of Microscope Resolution.

To quantify the lateral and axial resolution of the newly established microscope, it is important to quantify the Point Spread Function (PSF) of fluorescent point sources with proper Nyquist sampling. For this purpose, we use the method described in Supplementary Note 4 for casting an agarose cube with fluorescent nanospheres. Using the established parameters for a well-aligned ASLM acquisition, acquire a z-stack with a z-step that is ~1/2 to 1/3rd the size of the ideal axial resolution. Qualitatively, when visually inspecting the data, a well-aligned ASLM will have a symmetric, spherical PSF. For more quantitative measurements, several methods are available. First, with basic functionalities in Fiji, line profiles on beads can be retrieved and fitted with a Gaussian curve to extract the Full-Width Half-Maximum (FWHM) of the PSF, which is a commonly used metric for resolution. Alternatively, a very useful tool is the Fiji plugin MetroloJ (http://imagejdocu.tudor.lu/doku.php?id=plugin:analysis:metroloj:start), which provides a detailed report for the PSF of a selected bead in 3D. By selecting several beads throughout the field of view, the quality of the light-sheet and uniformity of the resolution can be evaluated throughout a 3D volume. To automate this process, MetroloJ can be wrapped into a secondary macro or plugin that automatically iterates over selected portions of the whole 3D volume. Alternatively, we provide a MATLAB function that automatically measured the PSF dimensions throughout an entire volume on our GitHub repository (https://github.com/AdvancedImagingUTSW/manuscripts/tree/main/2021-dean-protocol).

SUPPLEMENTARY REFERENCES

21.   Voigt, F.F. et al. The mesoSPIM initiative: open-source light-sheet microscopes for imaging cleared tissue. *Nature Methods* **16**, 1105-1108 (2019).
46.   Hörl, D. et al. BigStitcher: reconstructing high-resolution image datasets of cleared and expanded samples. *Nature Methods* **16**, 870-874 (2019).
47.   Abrahamsson, S. et al. MultiFocus Polarization Microscope (MF-PolScope) for 3D polarization imaging of up to 25 focal planes simultaneously. *Opt Express* **23**, 7734-7754 (2015).